ORNL/TM-8467
Dist. Category UC-20 g

Contract No. W-7405-eng-26

ORNL/TM--8467

FUSION ENERGY DIVISION

DE83 012141

RESONANT ION TRANSPORT IN EBT

D. E. Hastings, E. F. Jaeger, and C. L. Hedrick
Fusion Energy Division

J. S. Tolliver
UCC-ND Computer Sciences

Date Published - May 1983

Prepared by the
OAK RIDGE NATIONAL LABORATORY
Oak Ridge, Tennessee 37830
operated by
UNION CARBIDE CORPORATION
for the
DEPARTMENT OF ENERGY

CONTENTS

ABSTRACT

We use a model for the ELMO Bumpy Torus as a bumpy cylinder with a toroidally induced vertical drift imposed on the plasma. With this model we obtain the neoclassical plasma-transport coefficients for ions in both the banana and plateau resonant regimes. The problem of solving the linearized bounce-averaged drift kinetic equation is formulated as a variational principle, which is shown to be valid for both the banana and plateau regimes. We use limiting forms of this principle to obtain a continuous collisionality approximation to the energy-dependent flux. We then use this approximation to obtain analytic formulae for the particle- and energy-diffusion coefficients. These are shown to give excellent agreement with numerical results.

I. INTRODUCTION

Recent measurements[1] of the ambipolar potential in the ELMO Bumpy Torus (EBT) have indicated that the potential drop is large ($\Delta\phi \sim 600$ eV) and gives a radial electric field that over most of the plasma points in a direction opposite to the radial magnetic field. In the case of ions, this leads to cancellations between the $\underline{E} \times \underline{B}$ drift and the poloidal components of the $\nabla\underline{B}$ and curvature drifts. Consequently, radial ion transport at low collisionalities is dominated by the particle orbits near the resonance[2,3] (i.e., the regions of phase space where the poloidal precession frequency becomes small). Two regimes can be distinguished in this limit of low collisionality: the plateau and banana regimes.[3] In the plateau regime,[4] collisions are sufficiently rapid to prevent completion of crescent orbits; however, the losses are still dominated by the localized region of velocity space where the resonant orbits occur. In the banana or crescent regime,[5] particles complete their crescent orbits before scattering and the diffusive step size then scales as the crescent width. The parameter of interest in determining whether the ions are in the plateau or banana regime is the collisionality ν_r/Ω_0 (where ν_r is the 90^o deflection frequency measured at the resonance and Ω_0 is the average poloidal gradient-B drift frequency). For $\nu_r/\Omega_0 \ll \delta^{3/2}$, where δ is the inverse aspect ratio (typically, $\delta \sim 0.1$ in EBT-S), the ions are in the banana regime. In the opposite limit, the ions are in the plateau regime. In the present EBT device it is difficult to understand a large potential drop in terms of the plateau diffusion coefficients. Experimentally, hot ions are observed, and it has been

conjectured that resonant particles in the hot ion distribution are responsible for the large potential. In order to evaluate this, it is necessary to have readily usable expressions for the diffusion coefficients that span the banana to plateau regime.

In this paper, we present a calculation of the neoclassical transport coefficients that spans both the banana and plateau regimes. Our diffusion coefficients are based upon a model of the EBT magnetic field that is a bumpy cylinder with a small toroidal correction. This is appropriate for the plasma core in a large aspect ratio EBT device but would not be appropriate near the high beta electron rings; however, the kinetic equation for the distribution function was derived independently of any model of the magnetic field. Our transport coefficients have a form that is convenient for use in computations of the time development of the radial profiles of density and temperature.[6]

In Sec. II, the basic equations are introduced. These include the linearized drift kinetic equation and the bounce-averaged vertical and poloidal drifts. In Sec. III, we review the work of Ref. 4 that is relevant to our work and correct a result derived there. We obtain the diffusion coefficients as integrals over the energy-dependent flux. In Sec. IV, we obtain the banana and Weiner-Hopf boundary layer[7] approximations to the energy-dependent flux and compare this result with a full numerical calculation of the energy-dependent flux. We then construct a continuous approximation to this flux valid for both the plateau and banana collisional regimes. In Sec. V, we use this approximation to obtain analytic formulae for the six diffusion

coefficients and compare these with the full numerical calculations of these coefficients. Finally, in Sec. VI, we summarize our results.

II. BASIC EQUATIONS

A. Resonant particle orbit model

In order to calculate the low collisionality ion transport rates it is necessary to have a drift orbit model that includes crescent-shaped orbits. The motion of particles parallel to the field lines in EBT is characterized either by circulation around the torus or by trapping between adjacent mirrors. For most of the particles in EBT the bounce time scale is much shorter than the time scale over which particles collide or drift off the flux surfaces. This being the case, it is desirable to average the rapid bounce motion since transport will occur on a much slower time scale. It has been shown[8] that if the longitudinal adiabatic invariant J is introduced then the bounce-averaged particles move on surfaces of constant J. Bounce-averaged components of the drift velocity $\vec{v}_d$ are given by

$$\langle \dot{\alpha} \rangle = \langle \vec{v}_d \cdot \nabla \alpha \rangle = \frac{1}{Ze\tau} \frac{\partial J}{\partial \beta} \tag{1a}$$

and

$$\langle \dot{\beta} \rangle = \langle \vec{v}_D \cdot \nabla \beta \rangle = - \frac{1}{Ze\tau} \frac{\partial J}{\partial \alpha} \ , \tag{1b}$$

where

$$J = m \oint d\ell v_{\parallel} \quad , \tag{2}$$

$$\tau = \oint \frac{d\ell}{v_{\parallel}} \quad , \tag{3}$$

$$v_{\parallel} = \left(\frac{2}{m}\right)^{1/2} \left(\varepsilon - Ze\phi - \mu B\right)^{1/2} \quad , \tag{4}$$

$$\varepsilon = \frac{1}{2} m v^2 + Ze\phi \quad , \tag{5}$$

$$\mu = \frac{m v_{\perp}^2}{2B} \quad , \tag{6}$$

and α and β are standard magnetic field coordinates (eg., α could be a flux variable and β, a poloidal angle) such that $\vec{B} = \nabla\alpha \times \nabla\beta$. Due to toroidal periodicity our analysis can be confined to a single EBT mirror sector; thus, the integrals in J and the bounce time τ are to be interpreted as being between mirror points for trapped particles and between coil planes for toroidally passing particles.

For our purposes we are interested in regions of phase space where the bounce-averaged poloidal precession frequency $\Omega \equiv \langle \dot{\beta} \rangle$ is small. When Ω passes through zero, a precessing particle will change directions and can, if in a sufficiently collisionless plasma, execute banana- or crescent-shaped orbits. Particles on such orbits will be referred to as "banana trapped" or simply "trapped." The notation

"untrapped" or "passing" will refer to particles that do not execute banana orbits. There should be no confusion between poloidal and toroidal directions since this analysis makes no distinction between toroidally passing and toroidally mirror-trapped particles except in the calculations of J and τ mentioned above. The drift frequency Ω as well as the "radial" drift velocity $V \equiv \langle \dot{\alpha} \rangle$ can be calculated from Eq. (1) once a model magnetic field is assumed. We note at this point that $\langle \dot{\alpha} \rangle$ does not have the dimensions of a true radial drift velocity since α is regarded as a flux surface coordinate $\sim r^2 B$. However, as in Ref. 5, since α measures the minor radius of the plasma, we shall refer to it as a "radial" coordinate.

The radial width of a collisionless orbit, $\Delta\alpha$, is approximately given by

$$\Delta\alpha \sim \left| \frac{\langle \dot{\alpha} \rangle}{\langle \dot{\beta} \rangle} \right| \quad . \tag{7}$$

For passing particles

$$\frac{\Delta\alpha}{\Delta\alpha_m} \sim \delta << 1 \quad , \tag{8}$$

where $\delta = r/R_T$ is the inverse aspect ratio and $\Delta\alpha_m$ is the equilibrium length scale. However, for particles that execute crescent-shaped orbits such that for a fixed "radial" location α_0, $\Omega = 0$, the "radial" width in Eq. (7) may become very large.[5] This observation is of importance in the linearization of the drift kinetic equation.

To obtain a model for J, $\langle\dot{\alpha}\rangle$, and $\langle\dot{\beta}\rangle$, we first make the observation that particles move on drift surfaces (of constant J) rather than on flux surfaces (of constant α). Thus, we shall later want to transform from an (α,β) coordinate system to a (J,β) coordinate system. In what follows, we have been strongly motivated by the analysis in Refs. 9 and 5. Let us first make the assumption that the transport coefficients can be treated as local quantities and expand the α-dependence of J about a fixed "radial" position $\alpha = \alpha_0$:

$$J(\alpha,\beta) = J(\alpha_0,\beta) + \left(\frac{\partial J}{\partial \alpha}\right)_{\alpha_0}(\alpha - \alpha_0) + \frac{1}{2}\left(\frac{\partial^2 J}{\partial \alpha^2}\right)_{\alpha_0}(\alpha - \alpha_0)^2 + \ldots . \quad (9)$$

Since the poloidal variation of Ω on a flux surface is weak, we can expand Ω about α_0 and neglect the β-dependence:

$$\Omega(\alpha,\beta) \approx \Omega^0(\alpha_0) + \Omega^{0\prime}(\alpha_0)(\alpha - \alpha_0) \quad . \quad (10)$$

Here, the superscript zero means that Ω^0 is evaluated in the infinite aspect ratio ($\delta = 0$) bumpy cylinder limit; this accomplishes the neglect of the β-dependence. The prime means an α-derivative. With this approximation,

$$\left(\frac{\partial J}{\partial \alpha}\right)_{\alpha_0} = -Ze\tau\Omega(\alpha_0,\beta) = -Ze\tau\Omega^0(\alpha_0) \quad (11)$$

and

$$\left(\frac{\partial^2 J}{\partial \alpha^2}\right)_{\alpha_0} \approx -Ze\tau\left(\frac{\partial \Omega}{\partial \alpha}\right)_{\alpha_0} = -Ze\tau\Omega^{0'}(\alpha_0) \quad , \tag{12}$$

where we have also neglected the α-dependence of τ. Inserting Eqs. (11) and (12) into Eq. (9), solving for $(\alpha - \alpha_0)$, and then inserting this result into Eq. (10), we find

$$\Omega(J,\beta) = \sigma\left\{(\Omega^0)^2 - \frac{2\Omega^{0'}}{Ze\tau}\left[J(\alpha,\beta) - J(\alpha_0,\beta)\right]\right\}^{1/2} \quad , \tag{13}$$

where $\sigma = \Omega/|\Omega| = \pm 1$.

For the β-dependence of J, we assume from symmetry that β enters only as $\cos\beta$. Then, for $\alpha = \alpha_0$, we write

$$J(\alpha_0,\beta) = J_0 - x_0\cos\beta \tag{14}$$

where x_0 is to be determined. Defining

$$V_y \equiv -\frac{1}{Ze\tau}\frac{\partial J}{\partial(\cos\beta)} \quad , \tag{15}$$

so that

$$V_{y0} \equiv V_y(\alpha_0) = -\frac{1}{Ze\tau}\frac{\partial J(\alpha_0,\beta)}{\partial(\cos\beta)} = \frac{x_0}{Ze\tau} \tag{16}$$

we see that $x_0 = Ze\tau V_{y0}$. We note the following relationship between V and V_y:

$$\langle \dot{\alpha} \rangle = V = \frac{1}{Ze\tau} \frac{\partial J}{\partial \beta} = V_y \sin \beta \quad . \tag{17}$$

We refer to V_y as the "vertical" drift due to toroidicity (i.e., finite aspect ratio) but recall that neither V nor V_y has units of m/s. From Eqs. (14) and (16) we can write

$$J(\alpha, \beta) - J(\alpha_0, \beta) = J - J_0 + Ze\tau V_{y0} \cos \beta \quad .$$

Then, Eq. (13) becomes

$$\Omega(J, \beta) = \sigma\{(\Omega^0)^2 - \frac{2\Omega^{0'}}{Ze\tau} [J - J_0 + Ze\tau V_{y0}(\cos \beta)]\}^{1/2} \quad . \tag{18}$$

Defining

$$J_* = (\Omega^0)^2 - \frac{2\Omega^{0'}}{Ze\tau}(J - J_0) \tag{19}$$

and

$$J_c = 2\Omega^{0'} V_{y0} \quad , \tag{20}$$

then

$$\Omega(J, \beta) = \sigma(J_* - J_c \cos \beta)^{1/2} \quad . \tag{21}$$

$$\langle \dot{\alpha} \rangle = V = \frac{1}{Ze\tau} \frac{\partial J}{\partial \beta} = V_y \sin \beta \quad . \tag{17}$$

We refer to V_y as the "vertical" drift due to toroidicity (i.e., finite aspect ratio) but recall that neither V nor V_y has units of m/s. From Eqs. (14) and (16) we can write

$$J(\alpha, \beta) - J(\alpha_0, \beta) = J - J_0 + Ze\tau V_{y0} \cos \beta \quad .$$

Then, Eq. (13) becomes

$$\Omega(J, \beta) = \sigma\{[(\Omega^0)^2 - \frac{2\Omega^{0'}}{Ze\tau} [J - J_0 + Ze\tau V_{y0}(\cos \beta)]\}^{1/2} \quad . \tag{18}$$

Defining

$$J_* = (\Omega^0)^2 - \frac{2\Omega^{0'}}{Ze\tau}(J - J_0) \tag{19}$$

and

$$J_c = 2\Omega^{0'} V_{y0} \quad , \tag{20}$$

then

$$\Omega(J, \beta) = \sigma(J_* - J_c \cos \beta)^{1/2} \quad . \tag{21}$$

Equations (17) and (19) give the expressions for $\langle\dot{\alpha}\rangle$ and $\langle\dot{\beta}\rangle$ to be used later.

So far all the "radial" information is contained in α. No mention of a true radial coordinate has been made. For our later analysis it will be convenient to deal with drift velocities that have the correct dimensions of m/s and with fluxes with dimensions of particles/m^2/s. To this end we need to define a true radial coordinate system (ρ,θ), where ρ = radius in the midplane and θ = poloidal angle. To calculate the Jacobian from (α,β) to (ρ,θ) we assume large aspect ratios and make the connections

$$\alpha \sim \psi = \int_0^\rho B_m(\rho')\rho' d\rho' \tag{22}$$

and

$$\beta \sim \theta \ , \tag{23}$$

where B_m is the magnetic field in the midplane. Then,

$$\vec{V}_d \cdot \nabla\alpha = \vec{V}_d \cdot \nabla\rho \frac{\partial\psi}{\partial\rho} = v_\rho \rho B_m \ . \tag{24}$$

Here, v_ρ is a true radial drift velocity. This gives

$$V_y = \frac{V}{\sin\theta} = \frac{\langle\vec{V}_d \cdot \nabla\alpha\rangle}{\sin\theta} = \frac{\langle v_\rho \rho B_m\rangle}{\sin\theta} \equiv \langle v_y\rangle \rho B_m \ , \tag{25}$$

where $\langle v_y \rangle = \langle v_\rho \rangle / \sin\theta$ is a true bounce-averaged vertical drift velocity. To first order in inverse aspect ratio, $\langle v_y \rangle$ has been given as[4]

$$\langle v_y \rangle = v_{yth} w g(\zeta) \quad , \tag{26a}$$

where

$$v_{yth}(\rho) = -\frac{kT}{ZeB_m(\rho)R_T} \quad , \tag{26b}$$

$$w = \frac{mv^2}{2kT} \quad , \tag{27}$$

$$\zeta = \frac{v_\parallel}{v} \quad , \tag{28}$$

and for $\zeta < \zeta_-$, $g(\zeta)$ is given approximately by

$$g(\zeta) = 1 + \frac{1}{2}\zeta^2 \tag{29}$$

with

$$\zeta_- \equiv \frac{1}{\sqrt{2}} \left(1 - 4e^{-4}\right) \quad . \tag{30}$$

Here, we have assumed for simplicity that the poloidal electric field E_θ is zero. From Eqs. (16), (25), and (26) we have

$$V_{y0} = v_{y0} wg(\zeta) \rho_0 B_m(\rho_0) \quad , \tag{31a}$$

where

$$v_{y0} = v_{yth}(\rho_0) = \frac{-kT}{ZeB_m(\rho_0)R_T} \tag{31b}$$

and ρ_0 is the true radial location corresponding to the transport position $\alpha = \alpha_0$.

The bumpy cylinder bounce-averaged poloidal drift frequency has been given as[9]

$$\Omega^0 = \Omega_{th}[wh(\zeta) - w_0] \quad , \tag{32a}$$

where

$$\Omega_{th} = -\frac{kT}{ZeB_m(\rho)\rho R_c(\rho)} \quad , \tag{32b}$$

$$w_0 = -\frac{\Omega_E}{\Omega_{th}} \quad , \tag{33}$$

$$\Omega_E = -\frac{E_\rho}{\rho B_m} \quad , \tag{34}$$

$R_c(\rho)$ is the radius of curvature of the plasma, and E_ρ is the radial electric field. For $\zeta < \zeta_-$ the function $h(\zeta)$ is given approximately by

$$h(\zeta) = 1 - b\zeta^2 \quad , \tag{35}$$

where

$$b = \frac{1}{\zeta_-} \approx 2.33 \quad . \tag{36}$$

This expression for Ω^0 was derived in the limit $r \to 0$, and, consequently, the diffusion coefficients derived from it will be most valid near the centerline of the device. We have concentrated on the region of small pitch angle ζ because detailed analysis[4] has shown that the resonance region, $\Omega = 0$, occurs at much higher energies for particles that are not mirror trapped ($\zeta \approx 1$) than for mirror-trapped particles ($\zeta \approx 0$). Therefore, we shall assume that the primary contribution to the neoclassical diffusion coefficients comes from the mirror-trapped region of velocity space, and we shall concentrate our analyses there.

B. The bounce-averaged drift kinetic equation

We begin with the bounce-averaged steady-state drift kinetic equation as given earlier,[10]

$$\langle \dot{\alpha} \rangle \frac{\partial F}{\partial \alpha} + \langle \dot{\beta} \rangle \frac{\partial F}{\partial \beta} = C(F) \quad , \tag{37}$$

where C(F) is the bounce-averaged collision operator.

In Eq. (37) we make the transport ansatz and expand the distribution function about a Maxwellian. We then have

$$\langle \dot{\alpha} \rangle \left(\frac{\partial F_M}{\partial \alpha} + \frac{\partial f}{\partial \alpha}\right) + \langle \dot{\beta} \rangle \frac{\partial f}{\partial \beta} = C(f) \quad . \tag{38}$$

Since we want to be able to handle crescent-shaped orbits we must assume

$$\frac{\partial F_M}{\partial \alpha} \sim \frac{\partial f}{\partial \alpha} \quad ; \tag{39}$$

this comes from a consideration of Eqs. (7) and (8). In order to retain these wide crescent-shaped orbits we transform as anticipated in the derivation of Eq. (21) from $(\alpha, \beta, \varepsilon, \mu)$ coordinates to $(J, \beta, \varepsilon, \mu)$ coordinates. This is motivated by the observation that particles move on surfaces of constant J rather than on surfaces of constant α. We evaluate the equilibrium $\partial F_M/\partial \alpha$ at $\alpha = \alpha_0$ and designate it as $\partial F_M/\partial \alpha_0$ to obtain

$$C(f) - \langle \dot{\beta} \rangle \left.\frac{\partial f}{\partial \beta}\right|_J = \langle \dot{\alpha} \rangle \frac{\partial F_M}{\partial \alpha_0} \quad . \tag{40}$$

Now, we transform from $(J, \beta, \varepsilon, \mu)$ coordinates to $(J, \beta, \varepsilon, s)$ coordinates, where $s = \langle \dot{\beta} \rangle / \Omega_0$ and Ω_0 is a normalizing constant equal to Ω_{th} evaluated at the transport "radius" $\alpha = \alpha_0$. That is,

$$\Omega_0 = - \frac{kT}{ZeB_m(\rho_0)\rho_0 R_c(\rho_0)} \quad . \tag{41}$$

This transformation is motivated by the observation that the dominant ion transport comes from the region around the $\Omega = 0$ contour in phase space. The variable s is a dimensionless measure of the perpendicular distance from this $\Omega = 0$ contour. The kinetic equation then becomes

$$C(f) - \Omega_0 s \frac{\partial f}{\partial \beta} - \frac{J_c}{2\Omega_0} \sin \beta \frac{\partial f}{\partial s} = V_y \sin \beta \frac{\partial F_m}{\partial \alpha} \quad . \tag{42}$$

At this point we must give an explicit form for C(f). This operator may be significantly simplified by using the fact that the dominant ion transport comes from the region near the resonance. Hence, we can write[4]

$$C(f) = \nu(\varepsilon,\mu) \frac{\partial^2 f}{\partial s^2} \quad . \tag{43}$$

The form of $\nu(\varepsilon,\mu)$ was derived in Ref. 4 for EBT-I parameters with the bumpy cylinder magnetic field. From Ref. 4 we have, on transforming from (ε,μ) to (w,ζ),

$$\nu(w) = 4\nu_0 \left\{ 4wh^2(\zeta)D(w) + \frac{1}{2}E(w)w^{1/2}(1 - \zeta^2)[h'(\zeta)]^2 \frac{1 - 9/8\zeta^2}{1 - 3/4\zeta^2} \right\}_{s = 0} \tag{44}$$

where, at resonance {i.e., where $\Omega^0(\alpha = \alpha_0) = \Omega_0[wh(\zeta) - w_0] = 0$}, $v(w,\zeta)$ depends only on w since we can solve for

$$h = \frac{w_0}{w} \quad , \tag{45}$$

$$\zeta^2 = \left(\frac{1}{b}\right)\left(1 - \frac{w_0}{w}\right) \quad , \tag{46}$$

and

$$h' = -2\left[b\left(1 - \frac{w_0}{w}\right)\right]^{1/2} \quad . \tag{47}$$

In Eq. (44),

$$D(w) = \frac{1}{4w^{3/2}}\left[\frac{\sqrt{\pi}}{2}\,\mathrm{erf}(w^{1/2}) - w^{1/2}\exp(-w)\right]$$

$$+ \frac{1}{4\alpha_1 w^{3/2}}\left[\frac{\sqrt{\pi}}{2}\,\mathrm{erf}(\sqrt{\alpha_1}w^{1/2}) - \sqrt{\alpha_1}w^{1/2}\exp(-\alpha_1 w)\right] \quad , \tag{48}$$

$$E(w) = \frac{1}{2}\left\{\left(1 - \frac{1}{2w}\right)\left[\frac{\sqrt{\pi}}{2}\,\mathrm{erf}(w^{1/2})\right] - w^{1/2}\exp(-w) + w^{1/2}\exp(-w)\right\}$$

$$+ \frac{1}{2}\left\{\left(1 - \frac{1}{2\alpha_1 w}\right)\left[\frac{\sqrt{\pi}}{2}\,\mathrm{erf}(\sqrt{\alpha_1}w^{1/2}) - \sqrt{\alpha_1}w^{1/2}\exp(-\alpha_1 w)\right]\right.$$

$$\left. + \sqrt{\alpha_1}w^{1/2}\exp(-\alpha_1 w)\right\} \quad , \tag{49}$$

$$\alpha_1 = \left(\frac{m_e}{m_i}\right)\left(\frac{T_i}{T_e}\right) \quad , \tag{50}$$

and

$$\nu_0 = \frac{\sqrt{2}\pi\, ne^4 \ell n\, \Lambda}{m_i^{1/2}(kT_i)^{3/2}} \quad . \tag{51}$$

This collision frequency contains both ion-ion and ion-electron collisions across the resonance region. In asymmetric systems like EBT, both like and unlike collisions contribute to transport.

Finally, we transform from (J,β,ε,s) to (J,β,ε,z), where $z = [\nu(w)/\Omega_0]^{-1/3}s$. This is motivated by the observation that in the plateau regime the width of the collisional boundary layer about $s = 0$ is $O[(\nu/\Omega_0)^{-1/3}]$. Then, the collision operator becomes

$$C(f) = \nu(w)\,\frac{\partial^2 f}{\partial s^2} = \nu\left(\frac{\Omega_0}{\nu}\right)^{2/3}\frac{\partial^2 f}{\partial z^2} \quad ,$$

and Eq. (42) becomes

$$\frac{\partial^2 f}{\partial z^2} - z\,\frac{\partial f}{\partial \beta} - y\,\sin\beta\,\frac{\partial f}{\partial z} = V_y \sin\beta\,\frac{1}{\Omega_0}\left(\frac{\nu}{\Omega_0}\right)^{-1/3}\frac{\partial F_M}{\partial \alpha_0} \quad , \tag{52}$$

where

$$y(w) \equiv \frac{J_c}{2\Omega_0^2}\left[\frac{\nu(w)}{\Omega_0}\right]^{-2/3} \tag{53}$$

and is to be evaluated at resonance. From Eq. (20) for J_c it is clear that y has the sign of $\Omega^{0\prime}V_{y0}$, which is positive for bananas located on the inside of the torus and negative for bananas on the outside of the torus. It is convenient at this point to make the choice $\Omega^{0\prime}V_{y0} > 0$ so that y is a positive number. We follow the detailed discussion in Ref. 3 and observe that plateau behavior is obtained when the first two terms on the left-hand side and the right-hand side are balanced against each other so that the singularity at z = 0 is resolved by collisions and that banana or crescent behavior is obtained when the singularity at z = 0 is resolved by balancing the last two terms on the left-hand side and the right-hand side. In terms of the parameter y (as far as this kinetic equation is concerned), $y << 1$ gives the plateau regime whereas $y >> 1$ gives the banana regime. To simplify Eq. (52) we write it as

$$\frac{\partial^2 f'}{\partial z^2} - z\frac{\partial f'}{\partial \beta} - y \sin\beta \frac{\partial f'}{\partial z} = \sin\beta \ , \tag{54}$$

where

$$f = f'\left[V_y \frac{\partial F_M}{\partial \alpha_0}\frac{1}{\Omega_0}\left(\frac{\nu}{\Omega_0}\right)^{-1/3}\right] \ . \tag{55}$$

Finally, we write $f' = f^+ + f^-$ (the even and odd parts, respectively, with respect to z) to obtain

$$\frac{\partial^2 f^+}{\partial z^2} - z\frac{\partial f^-}{\partial \beta} - y \sin\beta \frac{\partial f^-}{\partial z} = \sin\beta \quad , \tag{56a}$$

and

$$\frac{\partial^2 f^-}{\partial z^2} - z\frac{\partial f^+}{\partial \beta} - y \sin\beta \frac{\partial f^+}{\partial z} = 0 \quad . \tag{56b}$$

These are the "stripped" drift kinetic equations on which we shall perform our analysis. We remark that these kinetic equations were derived without any assumptions about the magnetic field and so we expect them to be valid for both the core plasma and the reversed gradient region at the ring.

The domain of Eqs. (56a) and (56b) is $z \in (-\infty,+\infty)$ and $\beta \in [-\pi,\pi]$. For purposes of numerical calculation, this domain can be reduced. A reduction in the z-direction to $z \in [0,\infty)$ is obvious from the symmetry properties of f^+ and f^- in z. A reduction in the β-direction is possible because a further decomposition of both f^+ and f^- into even and odd parts in β reveals that f^+ can have no even part in β and that f^- can have no odd part in β. In summary, f^+ is even in z and odd in β whereas f^- is odd in z and even in β. Therefore, from these symmetry properties, we only require knowledge of f^+ and f^- on the restricted domain $z \in [0,\infty)$ and $\beta \in [0,\pi]$.

It is also important to note that the transformation

$$f^+(z,\beta) \to -f^+(z,\beta+\pi) \quad ,$$

$$f^-(z,\beta) \to -f^-(z,\beta+\pi) \quad ,$$

and

$$y \to -y$$

yields equations identical to Eqs. (56a) and (56b). That is, a choice of $\Omega^{0'} v_{y0} < 0$ (such that bananas occur on the outside of the torus and y is negative) corresponds mathematically to an inversion and a translation along β by π. It will be shown later that the quantity of interest for flux calculations is proportional to

$$\int_{-\pi}^{\pi} d\beta \; sw\beta f^+ = 2\int_{0}^{\pi} d\beta \; sw\beta f^+ \quad .$$

From the symmetry properties of f^+ and $sw\beta$ and the behavior of f^+ for negative y, it is clear that this quantity is invariant under the transformation $y \to -y$. This result is very convenient since it means that we can perform all of our analysis upon the assumption $y > 0$ and then replace y with $|y|$ in the final formulas to allow for the possibility that J_c is negative rather than positive.

III. THE VARIATIONAL PRINCIPLE

Spong and Hedrick[4] show that a variational principle for Eqs. (56a) and (56b) valid for arbitrary y is

$$S[f^+, f^-] = -\frac{J_- J_D^2}{J_+ J_- + (J_B + yJ_A)^2} \quad , \tag{57a}$$

where

$$J_D = \int_{-\infty}^{\infty} dz \int_{-\pi}^{\pi} d\beta \sin \beta f^+ \quad , \tag{57b}$$

$$J_B = \int_{-\infty}^{\infty} dz \int_{-\pi}^{\pi} d\beta \, z f^+ \frac{\partial f^-}{\partial \beta} \quad , \tag{57c}$$

$$J_A = \int_{-\infty}^{\infty} dz \int_{-\pi}^{\pi} \sin \beta \, d\beta \, f^+ \frac{\partial f^-}{\partial z} \quad , \tag{57d}$$

and

$$J_\pm = \int_{-\infty}^{\infty} dz \int_{-\pi}^{\pi} d\beta \, f^\pm \frac{\partial^2 f^\pm}{\partial z^2} \quad . \tag{57e}$$

There has been some confusion in the literature[3] as to whether the variational principle $\delta S = 0$ does indeed apply for all y. We emphasize that the kinetic Eqs. (56a) and (56b) contain all the information

about the wide excursions of the crescent-shaped orbits. This was retained by transforming from $(\alpha,\beta,\varepsilon,\mu)$ to $(J,\beta,\varepsilon,\mu)$ variables, and since $\delta S = 0$ does reproduce these kinetic equations for any y, it must apply for all y. The confusion arises from the formal similarity of Eq. (54) to the plateau equation for axisymmetric tokamaks.[7] We note that here the derivatives on β are to be understood as being at constant J and not at constant α.

In Ref. 4, it is shown that when the correct solutions to the kinetic equation are used then S reduces to

$$S = -J_D = -\int_{-\infty}^{\infty} dz \int_{-\pi}^{\pi} d\beta \sin \beta f^{+} \quad . \tag{58}$$

This quantity is related to the energy-dependent flux. In particular, with the particle (Γ_n) and energy (Γ_E) fluxes given by

$$\Gamma_n = \oint \frac{d\beta}{2\pi} \int d^3v \, \langle \dot{\alpha} \rangle f \tag{59}$$

and

$$\Gamma_E = \oint \frac{d\beta}{2\pi} \int d^3v \langle \dot{\alpha} \rangle (\tfrac{1}{2} mv^2) f \quad , \tag{60}$$

if we transform from $(\beta,\underline{v})$ to (β,w,z) and integrate along the resonance, we get

$$\Gamma_n = -\left(\frac{2kT}{m}\right)^{3/2} \int_{w_0}^{\infty} w^{-1/2} dw \left[\frac{1}{h'(\zeta)}\right]_{s=0} \left(\frac{\nu}{\Omega_0}\right)^{1/3} \int_{-\pi}^{\pi} d\beta \int_{-\infty}^{\infty} dz \langle\dot{\alpha}\rangle f \tag{61}$$

and

$$\Gamma_E = -\left(\frac{2kT}{m}\right)^{3/2} \int_{w_0}^{\infty} s^{-1/2} dw \left[\frac{1}{h'(\zeta)}\right]_{s=0} \left(\frac{\nu}{\Omega_0}\right)^{1/3} wkT \int_{-\pi}^{\pi} d\beta \int_{-\infty}^{\infty} dz \langle\dot{\alpha}\rangle f \quad . \tag{62}$$

When we substitute for $\langle\dot{\alpha}\rangle$ from Eq. (17) and Eq. (22) and for f from Eq. (55) and convert from flux in units of α to flux in units of ρ, we obtain

$$\Gamma_{\substack{n \\ \{E\}}} = \frac{1}{\Omega_0} \left(\frac{2kT}{m}\right)^{3/2} \int_{w_0}^{\infty} dw\, w^{-1/2} \frac{\partial F_M}{\partial \rho_0} \left[\frac{\langle v_y \rangle^2}{h'(\zeta)}\right]_{s=0} \left\{\frac{1}{wkT}\right\} \left[-J_D(w)\right] \quad . \tag{63}$$

Hence, we can calculate the particle and energy fluxes once we obtain J_D as a function of energy. For $y(w) << 1$, Spong and Hedrick calculated a second-order accurate solution for J_D by using the variational principle $\delta S = 0$.[4] We note some errors in their equations. Their Eq. (79) should be

$$I_1 = \frac{\sqrt{\pi}}{2} \frac{\Gamma(\frac{1}{6})}{\Gamma(\frac{2}{3})} \frac{\Gamma^2(\frac{2}{3})}{4(3^{2/3})}$$

while their Eq. (81) should be

$$I_2 = \frac{2}{3} I_3 = \frac{\pi}{4} (\frac{2}{3})^{2/3} \Gamma(\frac{1}{3}) \quad .$$

As a result, their $S^{(1)}$ becomes

$$S^{(1)} = \frac{\pi^2}{1 + 0.511y^2} \quad .$$

Hence, for $y << 1$, a second-order accurate solution for J_D is

$$J_D(w) = \frac{\pi^2}{1 + 0.511y^2(w)} \quad . \tag{64}$$

IV. THE ENERGY-DEPENDENT FLUX

In this section we will obtain a variationally accurate solution for $J_D(y)$ in the banana limit $y >> 1$ and compare our analytical results with the numerical solution of the kinetic equations. We start by defining a variable u by

$$z = \sqrt{u} - 2y \cos \beta \quad . \tag{65}$$

From a physical viewpoint, u is related to the β-independent part of $\langle\dot{\beta}\rangle$. We then have

$$\frac{\partial z}{\partial u} = \frac{1}{2z} , \quad \frac{\partial z}{\partial \beta} = \frac{y \sin \beta}{z} \quad . \tag{66}$$

We see that the tips of the crescent orbits occur for

$$\beta_c = \pm\cos^{-1}\left(\frac{u}{2y}\right) \quad . \tag{67}$$

We note that

$$z\frac{\partial f'}{\partial \beta}(u,\beta) = z\frac{\partial f'}{\partial \beta}(z,\beta) + y \sin \beta \frac{\partial f'}{\partial z}(z,\beta) \tag{68}$$

and

$$\frac{\partial^2 f'}{\partial z^2}(z,\beta) = 4z\frac{\partial}{\partial u}\left[z\frac{\partial}{\partial u} f'(u,\beta)\right] \quad . \tag{69}$$

The kinetic Eq. (54) then becomes

$$4z\frac{\partial}{\partial u}\left(z\frac{\partial}{\partial u}f'\right) - z\frac{\partial f'}{\partial \beta} = \sin \beta \quad . \tag{70}$$

We take out the particular solution $f' = -z/y$ to obtain the homogeneous equation

$$4\, z\frac{\partial}{\partial u}\left((u - 2y\cos\beta)^{1/2}\frac{\partial \tilde{f}}{\partial u}\right) - z\frac{\partial \tilde{f}}{\partial \beta} = 0 \quad , \tag{71}$$

where

$$f' = -\frac{z}{y} + \tilde{f} \quad . \tag{72}$$

The banana limit ($y >> 1$) occurs for $\nu \to 0$. In order to solve Eq. (71) in this small collisionality limit we return to the homogeneous form of Eq. (54). Since $y\sin\beta$ is not uniformly large for all values of β and large y, we must balance the last term on the LHS of Eq. (54) against either the first or second terms on the LHS. If the first term is chosen then the only solution which is regular everywhere in z and periodic in β is zero. Hence, we choose to balance the second and last terms on the LHS of the homogeneous form of Eq. (54) against each other. If we return to Eq. (42) and Eq. (43), we see that this corresponds to dropping the collision term C(f) which is consistent with our assumption of $y \to \infty$ because $\nu \to 0$. In addition, we will see later that a full numerical solution of Eqs. (56a) and (56b) for $y >> 1$ shows that the second derivative term in Eq. (54) is small everywhere except for the trapping boundary $u = 2y$. With these observations, we approximate Eq. (71) by expanding in the collisionality.

$$\tilde{f} = \tilde{f}_0 + \tilde{f}_1 \quad , \quad \tilde{f}_1 = O(\nu \tilde{f}_0) \quad . \tag{73}$$

$$- z\frac{\partial \tilde{f}_0}{\partial \beta} = 0 \tag{74}$$

and

$$4\, z\frac{\partial}{\partial u}\left(z\frac{\partial \tilde{f}_0}{\partial u}\right) - z\frac{\partial \tilde{f}_1}{\partial \beta} = 0 \quad . \tag{75}$$

From Eq. (74), we have

$$\tilde{f}_0 = g(u) \quad , \tag{76}$$

where g is an arbitrary function of u but independent of β. We can obtain the form of g by deriving a constraint equation from Eq. (75) in the following manner: for untrapped particles we must have single valuedness in β so that

$$\int_{-\pi}^{\pi} \frac{d\beta}{2\pi}\, \tilde{f}_1 = 0 \quad . \tag{77}$$

From Eq. (75), this gives

$$4 \int_{-\pi}^{\pi} \frac{d\beta}{2\pi} \frac{\partial}{\partial u}\left[z\frac{\partial}{\partial u}\, g(u)\right] = 0 \quad , \tag{78}$$

which implies

$$g'(u) = \frac{\text{constant}}{\oint z\,d\beta} \quad . \tag{79}$$

To evaluate the constant, we impose the condition that $\partial f'/\partial z \to 0$ for $z \to \infty$ to obtain from Eqs. (72) and (65)

$$0 = -\frac{1}{y} + \frac{\text{constant}}{\pi} \quad ,$$

which gives

$$g'(u) = \frac{\pi}{y} \frac{1}{\oint z\,d\beta} \quad \text{for } u \sim 2y \quad . \tag{80}$$

For particles that are on crescent orbits and do not sample the whole of the poloidal space we apply the operator

$$\sum_\sigma \frac{\sigma}{2} \int_{-\beta_c}^{\beta_c} d\beta$$

to $\partial \bar{f}_1/\partial\beta$ in order to obtain

$$\sum_\sigma \frac{\sigma}{2} \int_{-\beta_c}^{\beta_c} d\beta \frac{\partial \bar{f}_1}{\partial \beta} = \sum_\sigma \sigma[\bar{f}_1(\beta_c,\sigma) - \bar{f}_1(-\beta_c,\sigma)] \quad , \tag{81}$$

where $\sigma = z/|z|$. We note that as we integrate $\partial \bar{f}_1/\partial\beta$ are integrating around the banana orbit.

Since particles must be conserved at the banana tips we have

$$f'(\pm\beta_c, \sigma = +1) = f'(\pm\beta_c, \sigma = -1) \quad . \tag{82}$$

Hence, g(u) must be even in σ for trapped particles, and from Eqs. (81) and (75)

$$0 = \sum_{\sigma} \sigma \int_{-\beta_c}^{\beta_c} d\beta \; \frac{\partial}{\partial u}[zg'(u)]$$

$$= \frac{\partial}{\partial u}\{\int_{-\beta_c}^{\beta_c} z d\beta [g'(u, \sigma = +1) + g'(u, \sigma = -1)]\} \quad . \tag{83}$$

This implies that $g'(u)$ is odd in σ so that g(u) is odd in σ. Hence, for the trapped particles $|u| < 2y$, we must have

$$g(u) = 0 \quad . \tag{84}$$

Now, since our perturbed distribution function must be continuous, we integrate Eq. (80) from $u = 2y$:

$$f' = -\frac{z}{y} + \frac{\pi}{y} H(u - 2y) \int_{2y}^{u} \frac{du'}{\oint z' d\beta} \quad , \tag{85}$$

where H(x) is the Heaviside unit function and Eq. (85) is accurate to lowest order in collisionality. We now show that we can recover the banana constraint Eqs. (77) and (81) from the variational principle in Eq. (57a).

In the low collisionality regime ($\nu \to 0$) it is easy to see from Eq. (85) that f' to lowest order is odd in z. Hence, we must have

$$f^+ \lesssim O(\nu f^-) \quad . \tag{86}$$

It is easy to show that the variational principle $\delta S = 0$ is true if and only if

$$\delta J_D + \delta J_B + y\delta J_A + \frac{1}{2}(\delta J_- - \delta J_+) = 0 \quad . \tag{87}$$

From the definitions of the J's and using Eq. (86) we see that to lowest order in ν

$$\delta S = 0 \leftrightarrow \delta J_- = 0 \quad . \tag{88}$$

Hence, for small collisionality the variational quantity is J_-. It is easy to show from the kinetic equations that when J_- is evaluated on the correct solutions and evaluated to lowest order in ν J_D is obtained. Now, we have

$$0 = \delta J_- = \int_{-\infty}^{\infty} dz \int_{-\pi}^{\pi} d\beta \; \delta f^- \frac{\partial^2 f^-}{\partial z^2} \quad . \tag{89}$$

In Eq. (89) we change variables to (u,β). From Eqs. (72) and (76) we can write δf^- as a function of u alone; hence,

$$0 = \int_{-2y}^{2y} du\ \delta\bar{f}(u) \sum_{\sigma} \frac{\sigma}{2} \int_{-\beta_c}^{\beta_c} 2\frac{\partial}{\partial u}\left[z\frac{\partial}{\partial u}\, g(u)\right]d\beta$$

$$+ \int_{2y}^{\infty} du\ \delta\bar{f}(u) \int_{-\pi}^{\pi} d\beta\ 2\frac{\partial}{\partial u}\left[z\frac{\partial}{\partial u}\, g(u)\right]d\beta \quad . \tag{90}$$

In Eq. (90) we can vary $\delta\bar{f}(u)$ independently on the range $u \in [-2y,2y)$ and $u \in [2y,\infty)$. Then, it is easy to see that we recover precisely the banana constraint equations.

Since we have shown that the variational quantity for small ν is J_-, we evaluate this to obtain a variationally accurate estimate of J_D. We use Eq. (85) in J_- and obtain

$$J_- = -\frac{4\pi}{y^2} \int_{-2y}^{\infty} du \int_{-\pi}^{\pi} \delta(u - 2y)\frac{z^2}{\vartheta\ z d\beta}\, d\beta + \int_{2y}^{\infty} du \int_{-\pi}^{\pi} d\beta\ z\frac{\partial}{\partial u}\left(\frac{z}{\vartheta\ z d\beta}\right)$$

$$= -\frac{4\pi}{y^2}\left(\frac{\pi}{2}\, y^{1/2} - 0.193y^{1/2}\right) \quad . \tag{91}$$

In Eq. (91), the first term on the right-hand side arises from the δ function, which comes from differentiation of the step function H and physically manifests those particles that are on the boundary between being trapped in crescent orbits and untrapped. The second term was evaluated numerically and comes from the untrapped particles. The trapped particles give no contribution to this order.

We note that Eq. (19) can also be written as

$$J_- = -\frac{4\pi}{y} \lim_{u\to\infty} \int_{-\pi}^{\pi} \frac{f'(u,\beta)d\beta}{2\pi}$$

$$= -\frac{8\pi(0.69)}{y^{3/2}} \quad . \tag{92}$$

The Heaviside unit function arose because we did not treat the boundary layer at $u = 2y$ adequately. In order to remove this we use a Weiner-Hopf approach as in Ref. 7. We proceed as follows: in Eq. (70) we define functions $h_\pm$ by writing

$$f^+ = \frac{h_+ + h_-}{2} \tag{93}$$

and

$$f^- = -\frac{z}{y} + \frac{h_+ - h_-}{2} \quad ; \tag{94}$$

then, the functions $h_\pm$ satisfy

$$4\frac{\partial}{\partial u}\left(z\frac{\partial}{\partial u} h_\pm\right) = \pm \frac{\partial}{\partial \beta} h_\pm \quad . \tag{95}$$

The boundary conditions for f' are

$$u > |2y|: \quad f'(u,\beta = -\pi) = f'(u,\beta = \pi) \quad ,$$

and

$$u = 2y \cos\beta: \quad f'(\sigma = +1,\ \beta = \pm\beta_c) = f'(\sigma = -1,\ \beta = \pm\beta_c) \quad .$$

When written in terms of $h_\pm$ these reduce to

$$u = 2y \cos\beta: \qquad h_+ = h_- \quad , \tag{96}$$

$$u > 2y: \qquad h_\pm(u,\beta = 0) = h_\pm(u,\beta = 2\pi) \quad , \tag{97}$$

and

$$u << |2y|: \qquad h_\pm \to 0 \quad . \tag{98}$$

We wish to examine Eq. (95) near the trapping boundary $u = 2y$. We introduce a boundary layer variable x by

$$u = 2y - \lambda x \quad . \tag{99}$$

Then, $x < 0$ measures into the untrapped region and $x > 0$ measures into the trapped region. By the proper choice of λ, we can keep the highest derivative in the equation. Physically, this is appropriate since we expect that particles that go almost all the short way around the torus before reflecting and that spend a long time at the reflection points will be very susceptible to collisions. If we define

$$\phi = -\pi \cos \frac{\beta}{2} \quad , \tag{100}$$

then for $\lambda x << 1$ we obtain

$$\frac{8y^{1/2}}{\lambda^2} \sin\left(\frac{\beta}{2}\right) \frac{\partial^2}{\partial x^2} h_{\pm} - \frac{2}{\lambda^2} \frac{1}{y^{1/2}} \frac{\lambda}{\sin\left(\frac{\beta}{2}\right)} \frac{\partial}{\partial x} \left(x \frac{\partial h_{\pm}}{\partial x}\right) = \pm \frac{\pi}{2} \sin \frac{\beta}{2} \frac{\partial h_{\pm}}{\partial \phi} \quad . \tag{101}$$

The choice of $\lambda = (4/\pi^{1/2})y^{1/4}$ allows us to write

$$\frac{\partial^2 h_{\pm}}{\partial x^2} = \pm \frac{\partial h_{\pm}}{\partial \phi} \quad , \tag{102}$$

with these boundary conditions:

$$\text{(Trapped)} \qquad x > 0: \qquad h_{+} = h_{-} \text{ for } \phi = \pm \pi \quad , \tag{103}$$

$$x \to \infty: \qquad h_{\pm} \to 0 \quad , \tag{104}$$

and

$$\text{(Untrapped)} \qquad x < 0: \qquad h_{\pm}(-\pi) = h_{\pm}(\pi) \quad . \tag{105}$$

We have now written the problem in exactly the same form as the one solved in Ref. 7 by a Weiner-Hopf technique. We follow their analysis and obtain the same result; i.e., that the major effect of the boundary layer at $u = 2y$ is to add a constant $(1.21)A/2\pi$ to f' for $u > |2y|$ so as to correctly match the boundary layer region. The constant A is determined by matching $\partial h_+/\partial x$ as $x \to \infty$ with $\partial/\partial x \left(\frac{z}{y} + f'\right)$ as $u \to 2y_+$. This gives

$$A = \frac{\pi^{3/2}}{y^{5/4}} \quad , \tag{106}$$

such that for $u > |2y|$

$$f' = -\frac{z}{y} + \frac{(1.21)\pi^{1/2}}{2}\,\frac{1}{y^{5/4}} + \int_{2y}^{u} \frac{du'}{\oint z'd\beta} \quad . \tag{107}$$

If we now substitute this new form for f' into Eq. (92), we obtain the variationally accurate form for J_D with the boundary layer correction as

$$y(w) >> 1: \quad J_D = -\left[\frac{8\pi(0.69)}{y^{3/2}} - \frac{2(1.21)\pi^{3/2}}{y^{9/4}}\right] \quad . \tag{108}$$

We now have a variationally accurate solution for J_D for $y << 1$ [Eq. (64)] and for $y >> 1$ [Eq. (108)]. In order to evaluate the accuracy of these expressions, we have numerically solved the coupled Eqs. (56a) and (56b). Typical results are shown for $y << 1$ in Figs. 1(a)

and 1(b). In Figs. 1(a) and 1(b), we have $y = 0$ and see that most of the structure of f^+ and f^- is concentrated at $z = 0$, where collisions smooth the resonance and produce a boundary layer. In Figs. 2(a) and 2(b) we have f^+ and f^- plotted for $y = 10$. Now, we see that $f^+ << f^-$ as predicted and that the structure in f^+ occurs for $u = 2y$, i.e., $z = \sqrt{2y}(1 - \cos\beta)$. In Fig. 3(a) we have plotted $-J_C$ against $\nu_* \equiv y^{-3/2} = \nu[\Omega_0^2(W^{01}v_{y0})^{-3/2}]$, where J_D was evaluated four different ways. First, we evaluated it numerically using the numerical solutions for f^+. This was compared with J_D given in Eq. (64) (the plateau result), with J_D as given in Eq. (92) (the banana result), and with J_D as given in Eq. (108) (the banana result with a Weiner-Hopf correction). Figure 3(b) shows the relative errors in the three approximations to $-J_D$ as functions of y. We see that the corrected plateau result obtained in Ref. 4 gives a very good approximation for $y \lesssim 2$. The banana result is accurate for $y \gtrsim 8$. When the boundary layer correction is included, Eq. (108) is good for $y \gtrsim 1.8$. With this good agreement we can obtain an analytic approximation to $-J_D(y)$, which has at worst a 15% error (at $y = 1.93$) and is continuous if we write

$$-J_D(y) = \frac{\pi^2}{1 + 0.511y^2} \qquad 0 < |y| < 1.93 \tag{109}$$

and

$$-J_D(y) = \frac{8\pi(0.69)}{|y|^{3/2}} - \frac{2(1.21)\pi^{3/2}}{|y|^{9/4}} \qquad 1.93 \leq |y| \leq \infty \ , \tag{110}$$

where we have replaced y with |y| because of the arguments at the end of Sec. II.

V. THE DIFFUSION COEFFICIENTS

If we write the relationship between the fluxes and gradients as

$$\Gamma_n = -D_n \frac{dn}{d\rho} - D_T \frac{dT}{d\rho} + \mu_n n E_e \tag{111}$$

and

$$\Gamma_E = -K_n \frac{dn}{d\rho} - K_T \frac{dT}{d\rho} + \mu_T n E_\rho \ , \tag{112}$$

then with the use of Eq. (63) we can write the six transport coefficients as

$$D_n = \frac{\hat{D}_n}{\pi^2}\left(\frac{1}{2b} + 1\right)^2 \int_{w_0}^{\infty} \chi(w)dw \ , \tag{113}$$

$$D_T = \frac{n}{T}\frac{\hat{D}_n}{\pi^2}\left(\frac{1}{2b} + 1\right)^2 \int_{w_0}^{\infty} \chi(w)\left(w - \frac{3}{2}\right)dw \ , \tag{114}$$

$$K_n = kT\frac{\hat{D}_n}{\pi^2}\left(\frac{1}{2b} + 1\right)^2 \int_{w_0}^{\infty} dw\ w\chi(w) \quad , \tag{115}$$

$$K_T = kn\frac{\hat{D}_n}{\pi^2}\left(\frac{1}{2b} + 1\right)^2 \int_{w_0}^{\infty} dw\ w\left(w - \frac{3}{2}\right)\chi(w) \quad , \tag{116}$$

$$\mu_n = \frac{e}{kT}D_n ,$$

and

$$\mu_T = \frac{e}{kT} K_n \quad . \tag{117}$$

In these equations, we have

$$\hat{D}_n = \left(\frac{v_{y0}^2}{2\Omega_0}\right)\left(\frac{\pi}{b}\right)^{1/2} \tag{118}$$

and

$$\chi(w) = \frac{\exp(-w)}{(w - w_0)^{1/2}}\left[w - w_0 + \frac{w_0}{(1/2b + 1)}\right]^2 \{-J_D[y(w)]\} \quad . \tag{119}$$

From Eqs. (20), (31), and (53), we can obtain by evaluating v_{y0} and $\Omega^{0'}$ at the resonance to give

$$y(w) = \frac{\Delta}{2}\left(\frac{1}{2b} + 1\right)\left[\frac{\nu(w)}{\Omega_0}\right]^{-2/3}\left(w - w_0 + \frac{w_0}{1/2b + 1}\right) \quad , \tag{120}$$

where

$$\Delta = -2\delta\, \Omega^{0'}_{s=0}\, \left(\frac{kT}{\Omega_0^2 Ze}\right) = \frac{R_c}{r_d}\, \delta w_0 \quad , \tag{121}$$

$$\delta = \frac{\rho_0}{R_T} \, ,$$

and

$$\Omega^{0'}_{s=0} = -\frac{\Omega_E}{2r_d \rho_0 B_m(\rho_0)} \quad . \tag{122}$$

Here, r_d is the length scale over which Ω^0 varies at the resonance. The function $\nu(w)$ is obtained from Eq. (44). With the full w dependence of ν in Eq. (120) the integrals in Eqs. (113)–(116) are analytically intractable. In order to make some progress, we approximate y(w) in Eq. (120) by

$$y(w) = y_1(w - w_0 + \alpha_1) \quad , \tag{123}$$

where

$$\alpha_1 = \frac{w_0}{(\frac{1}{2b} + 1)} \quad , \tag{124}$$

$$y_1 = \frac{\Delta}{2}(\frac{1}{2b} + 1)(\frac{\bar{\nu}}{\Omega_0})^{-2/3} \quad , \tag{125}$$

and

$$\bar{\nu} = \int_{w_0}^{\infty} e^{-(w-w_0)} \nu(w) dw \quad . \tag{126}$$

The collision frequency $\bar{\nu}$ is clearly the weighted average of the full collision frequency along the resonance. This is motivated by the observation that for $y(w) >> 1$ and from Eqs. (120), (119), and (113)

$$D_n \sim \int_{w_0}^{\infty} e^{-w} \frac{(w - w_0 + \alpha)^{1/2}}{(w - w_0)^{1/2}} \nu(w) dw \quad .$$

If $w_0 << 1$ so that $\alpha_1 << 1$ and since $\nu(w)$ is an increasing function of energy,

$$D_n \sim \int_{w_0}^{\infty} e^{-w} \nu(w) dw = e^{-w_0} \bar{\nu} \quad .$$

This is precisely what is obtained by taking the approximate form for

$y(w)$ in Eq. (123). To allow for the possibility of $y < 0$ we simply insist that $y_1 > 0$ by placing absolute value signs around Δ in Eq. (125).

Let us define the integrals

$$L_n(w_0, \alpha_1, y_1) \equiv \int_{w_0}^{\infty} dw \exp(-w)(w - w_0)^{n-1/2}$$

$$\times (w - w_0 + \alpha_1)^2 \{-J_D[y_1(w - w_0 + \alpha_1)]\} \quad . \tag{127}$$

Here, we have formally treated w_0 and α_1 as independent variables. Now, the four diffusion coefficients can be written as

$$D_n = \frac{\hat{D}_n}{\pi^2} \left(\frac{1}{2b} + 1\right)^2 L_0 \quad , \tag{128}$$

$$D_T = \frac{n}{kT} \frac{\hat{D}_n}{\pi^2} \left(\frac{1}{2b} + 1\right)^2 [L_1 + (w_0 - \tfrac{3}{2})L_0] \quad , \tag{129}$$

$$K_n = kT \frac{\hat{D}_n}{\pi^2} \left(\frac{1}{2b} + 1\right)^2 (L_1 + w_0 L_0) \quad , \tag{130}$$

and

$$K_T = n\frac{\hat{D}_n}{\pi^2}\left(\frac{1}{2b} + 1\right)^2\left[L_2 + \left(2w_0 - \frac{3}{2}\right) L_1 + w_0\left(w_0 - \frac{3}{2}\right)L_0\right] \quad . \tag{131}$$

In Eq. (127) we transform from w to a new variable $z = y_1(w - w_0)$:

$$L_n = \frac{e^{-w_0}}{y_1^{n+5/2}} \int_0^\infty dz\, \exp(-z/y_1) z^{n-1/2}(z + \alpha_1 y_1)^2\left[-J_D(z + \alpha_1 y_1)\right] \quad . \tag{132}$$

For $\alpha_1 y_1 > 1.93$ we can use Eq. (110) and write

$$L_n = \frac{e^{-w_0}}{y_1^{n+5/2}} \left(M_{1n} - M_{2n}\right) \quad , \tag{133}$$

where

$$M_{1n} = 8\pi(0.69) \int_0^\infty dz\, \exp(-z/y_1) z^{n-1/2}(z + \alpha_1 y_1)^{1/2} \tag{134}$$

and

$$M_{2n} = 2(1.21)\pi^{3/2} \int_0^\infty dz\, \exp(-z/y_1) z^{n-1/2}(z + \alpha_1 y_1)^{-1/4} \quad . \tag{135}$$

From Ref. 11, the confluent hypergeometric function U(a,b,z) is defined as

$$U(a,b,z) = \frac{1}{\Gamma(a)} \int_0^\infty e^{-zt}\, t^{a-1}(1+t)^{b-a-1}dt \ , \quad \text{Re } b > \text{Re } a > 0 \ ,$$

and has the asymptotic expansion for $|z| >> 1$:

$$U(a,b,z) \sim z^{-a}\left[1 - \frac{a(1+a-b)}{z} + O\left(\frac{1}{z^2}\right)\right] \ .$$

We can now write M_{1n} and M_{2n} as

$$M_{1n} = 8\pi(0.69)(\alpha_1 y_1)^{n+1}\Gamma\left(n+\frac{1}{2}\right)U\left(n+\frac{1}{2},\ n+2,\ \alpha_1\right) \tag{136}$$

and

$$M_{2n} = 2(1.21)\pi^{3/2}(\alpha_1 y_1)^{n+1/4}\Gamma\left(n+\frac{1}{2}\right)U\left(n+\frac{1}{2},\ n+\frac{5}{4},\ \alpha_1\right) \ . \tag{137}$$

Now, we use the asymptotic expansion for the confluent hypergeometric function for $\alpha_1 >> 1$ and write for $\alpha_1 y_1 > 1.93$

$$L_0 \approx e^{-w_0}\left[\frac{8\pi^{3/2}(0.69)\alpha_1^{1/2}}{y_1^{3/2}}\left(1+\frac{1}{4\alpha_1}\right) - \frac{2(1.21)\pi^2}{y_1^{9/4}}\frac{1}{\alpha_1^{1/4}}\left(1-\frac{1}{8\alpha_1}\right)\right] \ . \tag{138}$$

For $y_1 << 1$ and for $\alpha_1 \sim O(1)$ we use Eq. (109) and write

$$L_0 \approx \frac{e^{-w}}{y_1^{5/2}} \int_0^{1.93-\alpha_1 y_1}$$

$$dz\ \exp(-z/y_1) z^{1/2} (z + \alpha_1 y_1)^2 \frac{\pi^2}{1 + 0.511(z + \alpha_1 y_1)^2} \quad . \qquad (139)$$

Since $y_1 << 1$ we can use Laplace's method[12] to asymptotically evaluate this integral as

$$L_0 \sim \frac{\pi_e^{2-w_0}}{y_1^{5/2}(1 + 0.511\alpha_1^2 y_1^2)} \sum_{k=0}^{\infty} \frac{(-1.01)^k (\alpha_1 y_1)^{k+2}}{(1 + 0.511\alpha_1^2 y_1^2)^k}$$

$$\times \int_0^{\infty} dz\ \exp(-z/y_1) z^{k-1/2} \left(1 + \frac{z}{\alpha_1 y_1}\right)^2 \left(1 + \frac{z}{2\alpha_1 y_1}\right)^k .$$

We now assume $\alpha_1 >> 1$ and linearize in $z/\alpha_1 y_1$. This is justified by noting that most of the contribution to the integrals comes from the neighborhood of $z = 0$. Then L_0 becomes

$$L_0 \sim \frac{\pi^2 e^{-w_0}}{1 + 0.511\alpha_1^2 y_1^2}$$

$$\times \sum_{k=0}^{\infty} \frac{(-1.01)^k \alpha_1^{k+2} y_1^{2k}}{(1 + 0.511\alpha_1^2 y_1^2)^k} \times \Gamma\left(k + \frac{1}{2}\right)\left[1 + \frac{1}{\alpha_1}\left(2 + \frac{k}{2}\right)\left(k + \frac{1}{2}\right)\right] .$$

(140)

We take k = 0 and k = 1, which gives the Padé approximant[13] $P_0^1(y_1^2)$, and construct the $P_1^0(y_1^2)$ approximant. Finally, we add the term arising from z^2 in Eq. (139) so that L_0 approaches the correct plateau limit for $\alpha_1 \sim O(1)$, and we obtain for $y_1 << 1$

$$L_0 \approx \frac{\pi^{5/2} e^{-w_0}}{1 + 0.511\alpha_1^2 y_1^2}\left(\alpha_1^2 + \alpha_1 + \frac{3}{4}\right) \frac{1}{1 + \left[\dfrac{(0.511)\alpha_1 y_1^2}{1 + 0.511\alpha_1^2 y_1^2}\right]} \frac{(1 + 15/4\alpha_1)}{(1 + 1/\alpha_1)} \, . \tag{141}$$

In Eq. (138) we have an approximation for L_0 for $y_1 > 1.93/\alpha_1$, and in Eq. (141) we have an approximation for L_0 for $y_1 << 1$.

We introduce a smoothing function

$$f_3(y_1) = \frac{1}{1 + (y_1/(1.93/\alpha_1))^3} \, . \tag{142}$$

This has the properties that

$$f(0) = 1 \, ,$$

$$f\left(\frac{1.93}{\alpha_1}\right) = \frac{1}{2} \, ,$$

and

$$f(\infty) = 0$$

and allows us to smoothly join the two limits for L_0. Hence, we write

$$L_0 = e^{-W_0}\left\{\frac{\pi^{5/2}(\alpha_1^2 + \alpha_1 + 3/4)}{1 + 0.511\,\alpha_1^2 y_1^2}\,\frac{f_3(y_1)}{1 + \dfrac{\alpha_1(0.511)y_1^2}{1 + 0.511\alpha_1^2 y_1^2}\,\dfrac{(1 + 15/4\alpha_1)}{(1 + 1/\alpha_1)}}\right.$$

$$\left. + [1 - f_3(y_1)]\left[\frac{8\pi^{3/2}(0.69)}{y_1^{3/2}}\left(1 + \frac{1}{4\alpha_1}\right) - \frac{2(1.21)}{y_1^{9/4}}\,\frac{\pi^2}{\alpha_1^{1/4}}\left(1 - \frac{1}{8\alpha_1}\right)\right]\right\} . \tag{143}$$

The diffusion coefficient D_n is then given by Eq. (128). In a similar manner we can construct L_1 and L_2, and we obtain

$$L_1 = e^{-W_0}\left\{\frac{\pi^{5/2}(\alpha_1^2 + 3\alpha_1 + 15/4)}{2(1 + 0.511\alpha_1^2 y_1^2)}\,\frac{f_3(y_1)}{1 + \dfrac{3\alpha_1(0.511)y_1^2(1 + 24/4\alpha_1)}{(1 + 0.511\alpha_1^2 y_1^2)(1 + 3/\alpha_1)}}\right.$$

$$\left. + [1 - f_3(y_1)]\left[\frac{4\pi^{3/2}(0.69)\alpha_1^{1/2}}{y_1^{3/2}}\left(1 + \frac{3}{4\alpha_1}\right) - \frac{(1.21)\pi^2}{\alpha_1^{1/4} y_1^{9/4}}\left(1 - \frac{3}{8\alpha_1}\right)\right]\right\} \tag{144}$$

and

$$L_2 = e^{-w_0}\left\{\frac{3\pi^{5/2}(\alpha_1^2 + 5\alpha_1 + 35/4)}{4\,(1 + 0.511\,\alpha_1^2 y_1^2)}\,\frac{f_3(y_1)}{1 + \dfrac{(0.511)5\alpha_1 y_1^2(1 + 35/4\alpha_1)}{1 + 0.511\alpha_1^2 y_1^2)(1 + 5/\alpha_1)}}\right.$$

$$\left. + [1 - f_3(y_1)]\left[\frac{6\pi^{3/2}(0.69)\alpha_1^{1/2}}{y_1^{3/2}}\left(1 + \frac{5}{4\alpha_1}\right) - \frac{3}{2}\,\frac{(1.21)\pi^2}{\alpha_1^{1/4} y_1^{3/4}}\left(1 - \frac{5}{8\alpha_1}\right)\right]\right\} . \tag{145}$$

The diffusion coefficients D_T, K_n, and K_T are then obtained from Eqs. (129)-(131).

In order to assess the accuracy of these analytic approximations we have computed the diffusion coefficients numerically and compared them to the analytic approximations. For these numerical computations the full functional form of $\nu(w)$ was used as given in Eq. (44). In addition, α_1 was evaluated from w_0 using Eq. (124). The parameter y_1 was written as

$$y_1\left(\frac{\nu_0}{\Omega_0}\right) = \frac{\delta}{2}\left(\frac{1}{2b} + 1\right)\left(\frac{\bar{\nu}_0}{\nu_0}\right)^{-2/3}\left(\frac{\nu_0}{\Omega_0}\right)^{-2/3} \tag{146}$$

and Δ was evaluated from Eq. (121) by taking $\delta = 0.1$ (the inverse aspect ratio typical of EBT-S) and choosing $(R_c/r_d) = 1$. The diffusion coefficients were then plotted against collisionality (ν_0/Ω_0) for several values of w_0. The range of collisionality was chosen to span the range of experimental interest for the hot ions observed in EBT. The values of w_0 were also chosen to span the range of experimental

interest. Typically, this is in the range $w_0 = 3$ to $w_0 = 7$. For $w_0 = 3$ we would expect that our analytic approximations might begin to break down since they were derived for $\alpha_1 >> 1$.

In Figs. 4(a)-4(d) we plot

$$\frac{D_n}{[\hat{D}_n\,(\frac{1}{2b}+1)^2\pi^{-2}e^{w_0}]}\,,\quad \frac{D_T}{[\frac{n}{kT}\,\hat{D}_n(\frac{1}{2b}+1)^2\pi^{-2}e^{w_0}]}\,,\quad \frac{K_n}{[kT\,\hat{D}_n(\frac{1}{2b}+1)^2\pi^{-2}e^{w_0}]}\,,$$

$$\frac{K_T}{[n\hat{D}_n\,(\frac{1}{2b}+1)^2\pi^{-2}e^{w_0}]}\,,$$

respectively, against (ν_0/Ω_0) for $w_0 = 3$. We compare our analytic approximation with the diffusion coefficients computed numerically in two ways: (1) from the numerical evaluation for $J_D(y)$ as given in Fig. 3 and (2) by using the analytic approximation to $J_D(y)$ as given in Eqs. (109) and (110). For each diffusion coefficient we see a plateau regime for large collisionality and a banana regime, where the diffusion coefficients increase with collisionality, for small collisionality. From Figs. 4(a)-4(d) we see that the analytic approximation reproduces the plateau results exactly. This is not surprising since here the diffusion coefficients are independent of collisionality. For the lower ranges of collisionality we see that the analytic approximation is worse for D_n, and even here it is only 6% larger than the numerically computed values. For D_T and K_T the analytic approximation is so good that it is hard to distinguish between the numerical and analytic curves. In Figs. 5(a)-5(d) we do

the same set of plots for $w_0 = 7$. Here, we do not see a plateau regime for the range of collisionality we consider. We note that the analytic approximations have the correct functional form as a function of (ν_0/Ω_0) but are slightly larger than the numerical calculations for all four diffusion coefficients. We attribute this to the fact that our approximation for $\nu(w)$ is breaking down for these large values of w_0.

Finally, we show that we can recover the familiar banana and plateau scalings from the analytic approximations. For simplicity, we shall concentrate on D_n.

We note that

$$y_1 = \delta \left(\frac{R_c}{r_d}\right)\frac{w_0}{2}\left(\frac{1}{2b} + 1\right)\left(\frac{\bar{\nu}}{\Omega_0}\right)^{-2/3} \quad ;$$

hence, the limit $y_1 >> 1$ corresponds to

$$\frac{\bar{\nu}}{\Omega_0 \delta^{3/2}} << \left[\left(\frac{R_c}{r_d}\right)\frac{w_0}{2}\left(\frac{1}{2b} + 1\right)\right]^{3/2} \quad .$$

The banana regime $y_1 << 1$ is then

$$D_n \sim \frac{8\sqrt{2}(0.69)\delta^{1/2}}{b^{1/2}}(R_c)^{1/2} r_d^{3/2} \frac{\nu e^{-w_0}}{w_0} \quad . \tag{147}$$

This has the familiar $\delta^{1/2}$ scaling with aspect ratio, the linear scaling with collision frequency, and the e^{-w_0} scaling with w_0 or electric field. The plateau regime $y_1 << 1$ is

$$D_n \sim \frac{\pi}{b^{1/2}} \delta^2 (R_c)^2 \frac{e^{-w_0}}{2} \Omega_0 \left[w_0^2 + w_0 \left(\frac{1}{2b} + 1 \right) + \frac{3}{4} \left(\frac{1}{2b} + 1 \right)^2 \right] \quad . \quad (148)$$

This has the familiar δ^2 scaling with aspect ratio, is independent of collisionality, and has the e^{-w_0} scaling with electric field.

We note that the banana result is dependent on the scale length in Ω^0 (i.e., r_d), and thus, when ambipolarity is imposed (i.e., $\Gamma_{ion} = \Gamma_{electron}$), a differential equation in the electric field will result, in contrast to the more well-known algebraic relationship for the electric field.[2] This is the subject of further study and will be reported on in a later paper. Preliminary results using these transport coefficients for the ions and improved trasnport rates for the electrons[14] indicate that large potential drops are possible although with somewhat larger ion tails than observed experimentally.

VI. CONCLUSIONS

For the bumpy cylinder magnetic field evaluated near the magnetic axis, we have solved the linearized drift kinetic equation for the banana and Weiner-Hopf approximations to the energy-dependent flux. We have used these with a corrected version of the plateau energy-dependent flux and have constructed analytic formulae for the particle and energy diffusion coefficients. For the ranges of electric field and collisionality of experimental interest we have shown that these formulae give excellent agreement with numerical results and can be used to compute the radial profiles of density and temperature.

REFERENCES

1. P. L. Colestock, K. A. Connor, and R. L. Hickok, Phys. Rev. Lett. 40, 1717 (1978).

2. E. F. Jaeger, C. L. Hedrick, and D. A. Spong, Nucl. Fusion 19, 1627 (1979).

3. R. D. Hazeltine, N. A. Krall, H. H. Klein, and P. J. Catto, Nucl. Fusion 19, 1597 (1979).

4. D. A. Spong and C. L. Hedrick, Phys. Fluids 23, 1903 (1980).

5. R. D. Hazeltine and P. J. Catto, Phys. Fluids 24, 290 (1981).

6. E. F. Jaeger, C. L. Hedrick, and W. B. Ard, Phys. Rev. Lett. 43, 885 (1979).

7. F. L. Hinton and M. N. Rosenbluth, Phys. Fluids 16, 836 (1973).

8. T. G. Northrop and E. Teller, Phys. Rev. 117, 215 (1960).

9. K. Tsang, "Banana Orbit Diffusion in EBT," in Proceedings of the EBT Transport Workshop, DOE-ET-0112, August 1979.

10. D. A. Spong, E. G. Harris, and C. L. Hedrick, Nucl. Fusion 19, 665 (1979).

11. M. Abramowitz and I. A. Stegun, Handbook of Mathematical Functions, NBS Applied Mathematics #5, p. 565.

12. C. M. Bender and S. A. Orszag, Advanced Mathematical Methods for Scientists and Engineers, McGraw-Hill (1978), p. 263.

13. C. M. Bender and S. A. Orszag, Advanced Mathematical Methods for Scientists and Engineers, McGraw-Hill (1978), p. 383.

14. D. E. Hastings and D. A. Spong, submitted to Physics of Fluids.

FIGURE CAPTIONS

FIG. 1. $-f^+$ and f^- are plotted against z and β for y = 0 in (a) and (b), respectively.

FIG. 2. $-f^+$ and f^- are plotted against z and β for y = 10 in (a) and (b), respectively.

FIG. 3. $-J_D$ is plotted against $y^{-3/2}$ for four different approximations to J_D in (a). Solid line is the numerical computation of J_D. Dashed line is the Spong and Hedrick corrected plateau approximation. Dotted line is the banana result, and dot-dash line is the banana result with Weiner-Hopf boundary layer correction. The relative error of the three approximations as compared to the numerical result is shown in (b).

FIG. 4. (a) $D_n/\left(\hat{D}_n\pi^{-2}\left(\frac{1}{2b}+1\right)^2 e^{W0}\right)$, (b) $D_T/\left(\frac{n}{kT}\hat{D}_n\left(\frac{1}{2b}+1\right)^2\pi^{-2}e^{W0}\right)$, (c) $K_n/\left(kT\hat{D}_n\left(\frac{1}{2b}+1\right)^2\pi^{-2}e^{W0}\right)$, and (d) $K_T/\left(n\hat{D}_n\left(\frac{1}{2b}+1\right)^2\pi^{-2}\ e^{W0}\right)$ are plotted against collisionality (ν_0/Ω_0) for W_0 = 3.

FIG. 5. (a) $D_n/\left(\hat{D}\pi^{-2}\left(\frac{1}{2b}+1\right)^2 e^{W0}\right)$, (b) $D_T/\left(\frac{n}{kT}\ D_n\left(\frac{1}{2b}+1\right)^2\ \pi^{-2}e^{W0}\right)$, (c) $K_n/\left(kT\hat{D}_n\left(\frac{1}{2b}+1\right)^2\pi^{-2}e^{W0}\right)$. and (d) $K_T/\left(n\hat{D}_n\left(\frac{1}{2d}+1\right)^2\ \pi^{-2}e^{W0}\right)$ are plotted against collisionality (ν_0/Ω_0) for W_0 = 7.

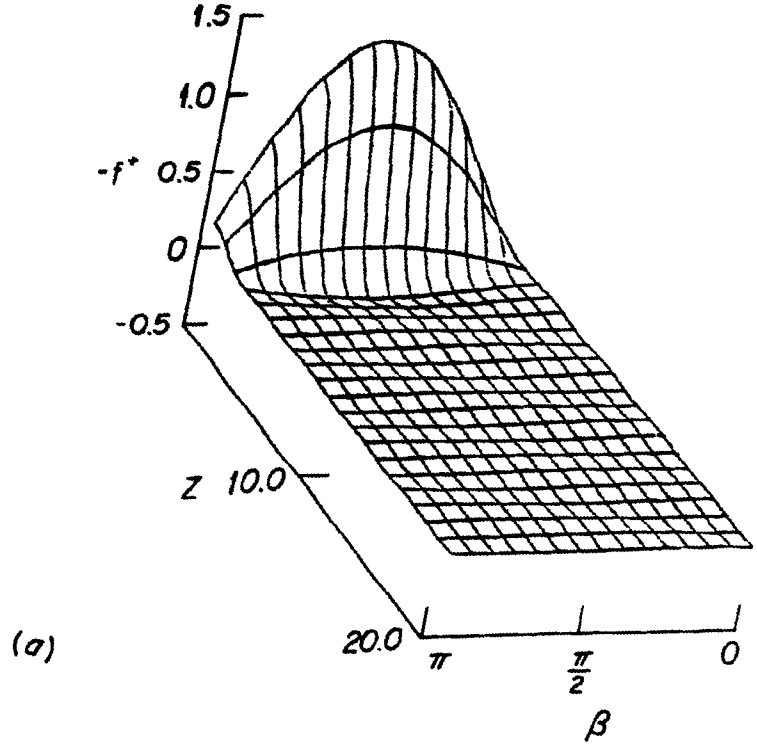
1.5
1.0
-f* 0.5
0
-0.5
Z 10.0
20.0
π
π/2
0
β

(a)

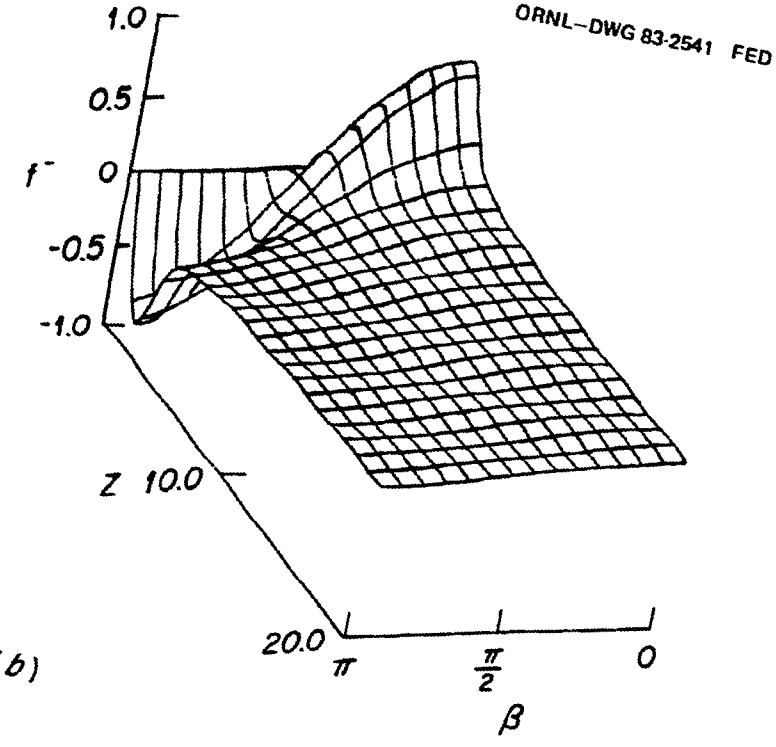
ORNL-DWG 83-2541 FED
1.0
0.5
f⁻ 0
-0.5
-1.0
Z 10.0
20.0
π
π/2
0
β

(b)

Fig. 1

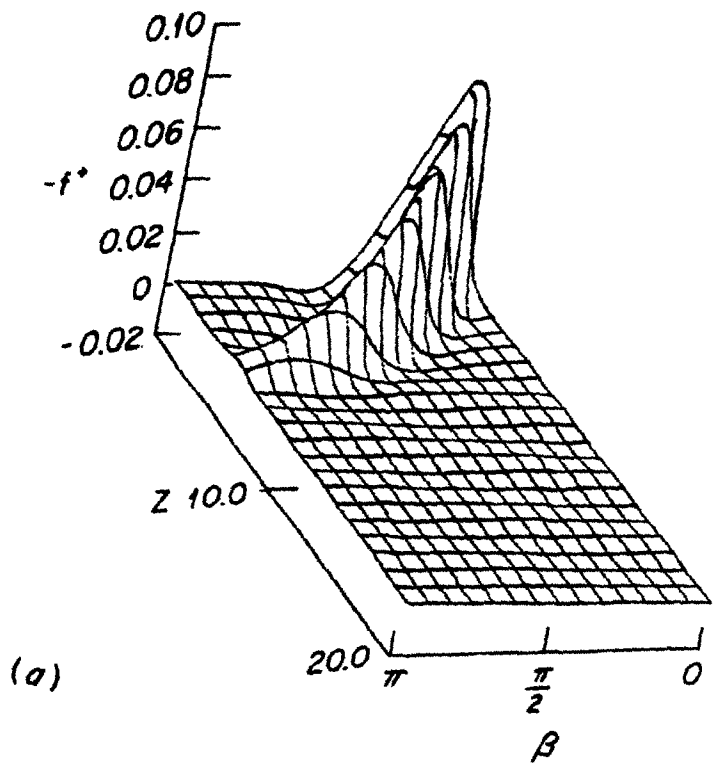
0.10
0.08
0.06
-f* 0.04
0.02
0
-0.02
Z 10.0
20.0
π
π/2
0
β

(a)

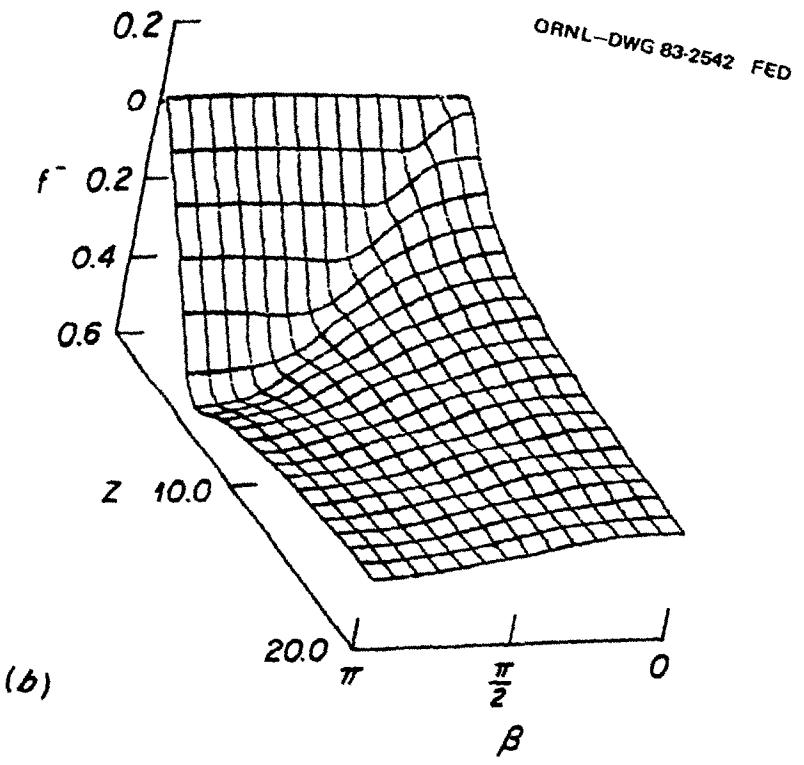
ORNL-DWG 83-2542 FED
0.2
0
f⁻ 0.2
0.4
0.6
Z 10.0
20.0
π
π/2
0
β

(b)

Fig. 2

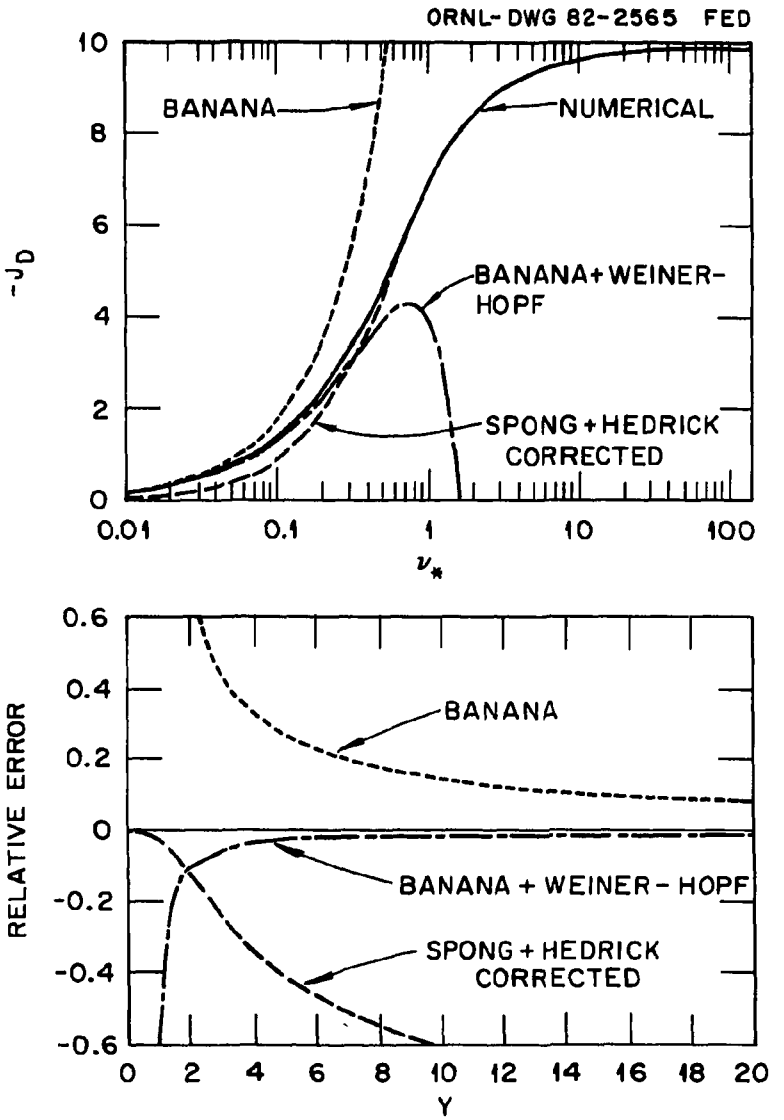
ORNL-DWG 82-2565 FED
BANANA
NUMERICAL
BANANA+WEINER-HOPF
SPONG+HEDRICK CORRECTED
$-J_D$
ν_*
RELATIVE ERROR
BANANA
BANANA + WEINER-HOPF
SPONG + HEDRICK CORRECTED
Y

Fig. 3

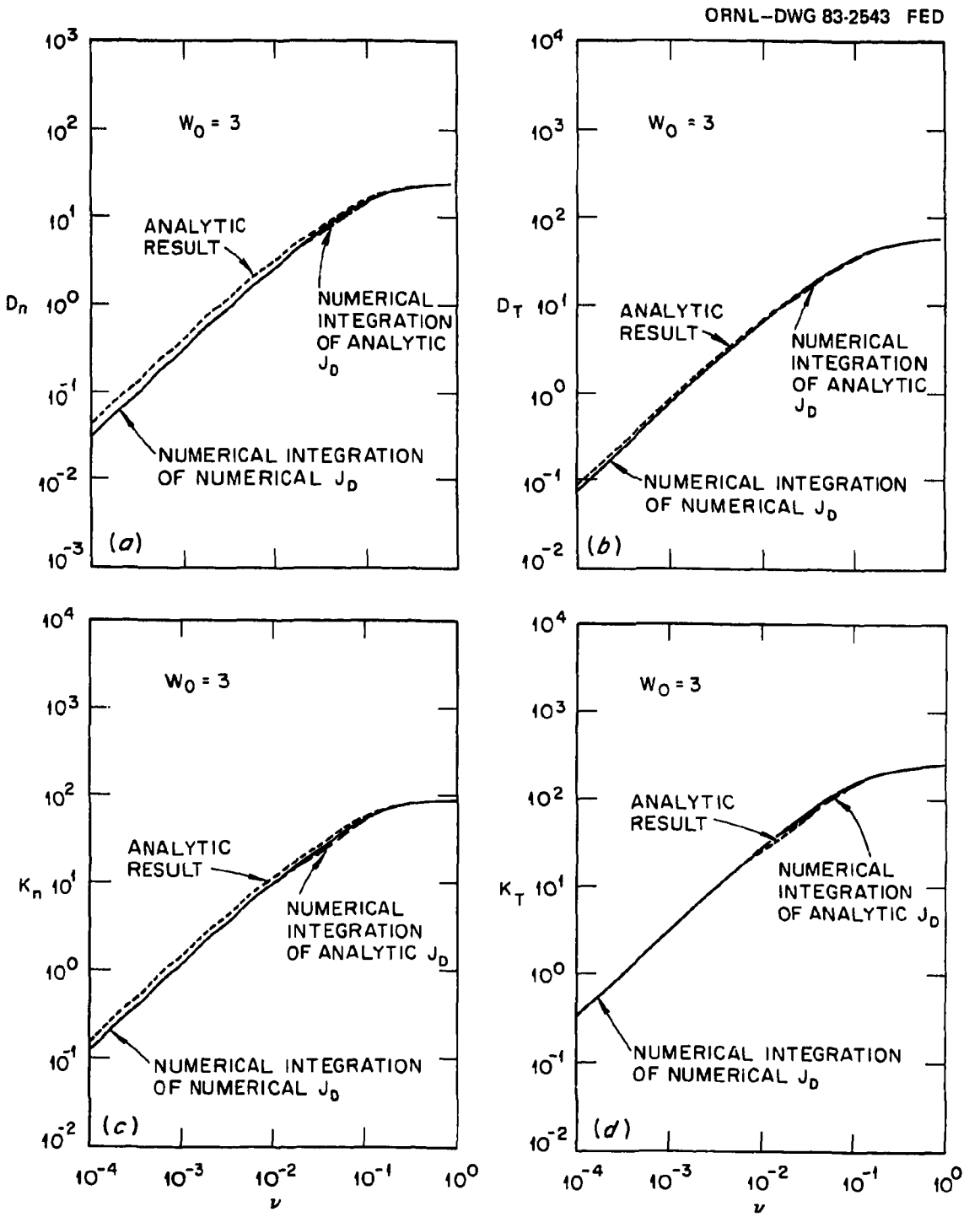
ORNL-DWG 83-2543 FED
$W_0 = 3$
ANALYTIC RESULT
NUMERICAL INTEGRATION OF ANALYTIC J_D
NUMERICAL INTEGRATION OF NUMERICAL J_D
D_n
D_T
K_n
K_T
(a)
(b)
(c)
(d)
ν

Fig. 4

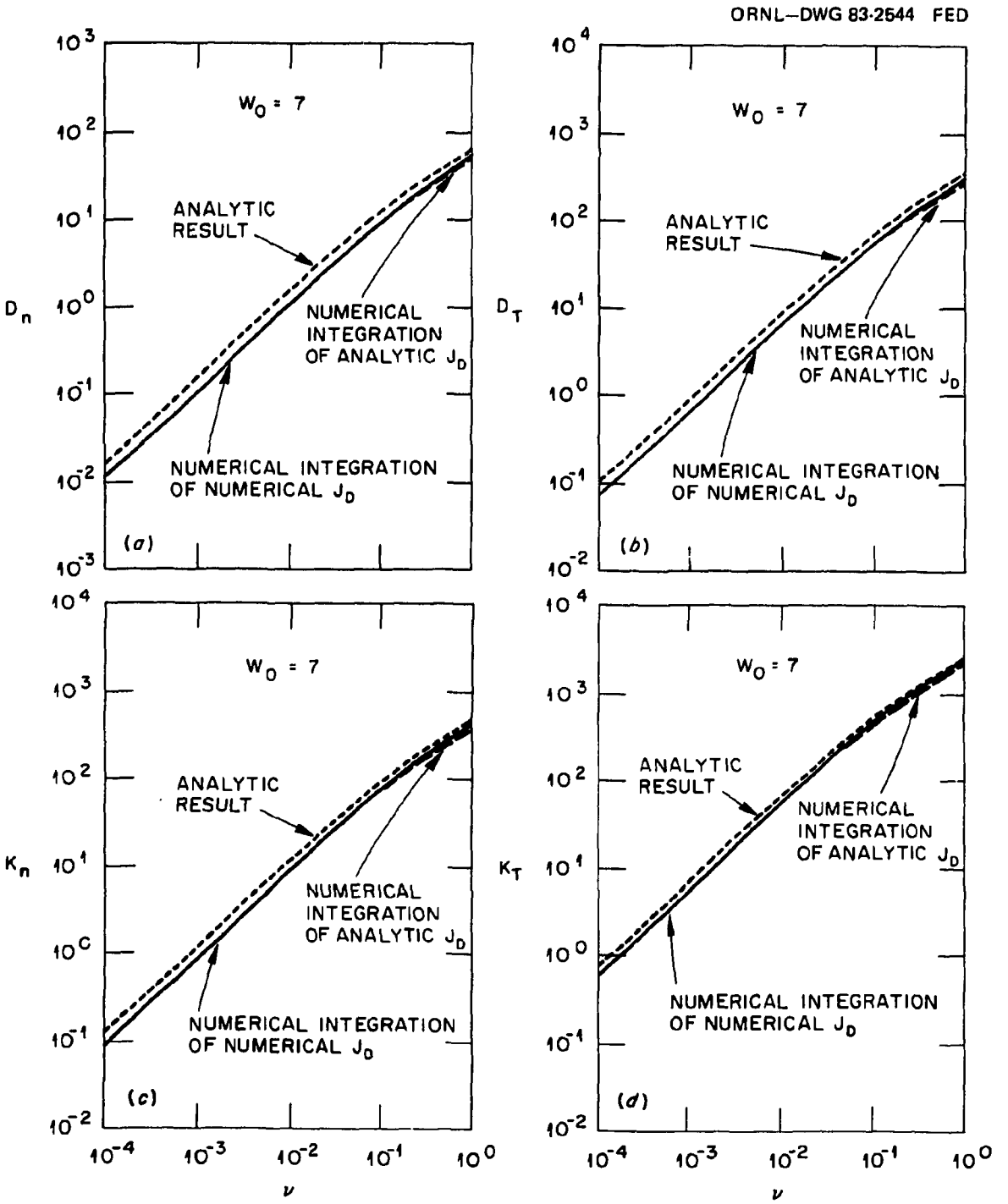
ORNL–DWG 83-2544 FED
$W_0 = 7$
ANALYTIC RESULT
NUMERICAL INTEGRATION OF ANALYTIC J_D
NUMERICAL INTEGRATION OF NUMERICAL J_D
D_n
D_T
K_n
K_T
(a)
(b)
(c)
(d)
ν

Fig. 5

ORNL/TM-8467
Dist. Category UC-20 g

INTERNAL DISTRIBUTION

1. W. A. Davis
2. T. Uckan
3. D. L. Hillis
4. S. Hiroe
5. H. O. Eason
6. J. K. Glowienka
7. F. W. Baity
8. J. Sheffield
9. R. A. Dory
10. D. B. Batchelor
11. N. A. Uckan
12. D. A. Spong
13. R. J. Colchin
14. L. Solensten
15. G. R. Haste
16-20. D. E. Hastings
21-25. E. F. Jaeger
26-30. C. L. Hedrick
31-35. J. S. Tolliver
36-37. Laboratory Records Department
38. Laboratory Records, ORNL-RC
39. Document Reference Section
40-41. Central Research Library
42. Fusion Energy Division Library
43. Fusion Energy Division Reports Office
44. ORNL Patent Office

EXTERNAL DISTRIBUTION

45. J. F. Clarke, Associate Director for Fusion Energy, Office of Fusion Energy, Office of Energy Research, Mail Stop G-256, U.S. Department of Energy, Washington, DC 20545
46. J. F. Decker, Director, Division of Applied Plasma Physics, Office of Fusion Energy, Office of Energy Research, Mail Stop G-256, U.S. Department of Energy, Washington, DC 20545
47. D. B. Nelson, Fusion Theory and Computer Services Branch, Office of Fusion Energy, Office of Energy Research, Mail Stop G-256, U.S. Department of Energy, Washington, DC 20545
48. M. N. Rosenbluth, RLM 11.218, Institute for Fusion Studies, University of Texas, Austin, TX 78712
49. W. Sadowski, Fusion Theory and Computer Services Branch, Office of Fusion Energy, Office of Energy Research, Mail Stop G-256, U.S. Department of Energy, Washington, DC 20545
50. A. Opdenaker, Reactor Systems and Applications Branch, Office of Fusion Energy, Office of Energy Research, Mail Stop G-256, U.S. Department of Energy, Washington, DC 20545
51. J. E. Baublitz, Reactor Systems and Applications Branch, Office of Fusion Energy, Office of Energy Research, Mail Stop G-256, U.S. Department of Energy, Washington, DC 20545
52. W. R. Ellis, Mirror Systems Branch, Office of Fusion Energy, Office of Energy Research, Mail Stop G-256, U.S. Department of Energy, Washington, DC 20545
53. J. M. Turner, Mirror Systems Branch, Office of Fusion Energy, Office of Energy Research, Mail Stop G-256, U.S. Department of Energy, Washington, DC 20545

54. T. V. George, Mirror Systems Branch, Office of Fusion Energy, Office of Energy Research, Mail Stop G-256, U.S. Department of Energy, Washington, DC 20545
55. N. A. Davies, Tokamak Systems Branch, Office of Fusion Energy, Office of Energy Research, Mail Stop G-256, U.S. Department of Energy, Washington, DC 20545
56. E. Oktay, Tokamak Systems Branch, Office of Fusion Energy, Office of Energy Research, Mail Stop G-256, U.S. Department of Energy, Washington, DC 20545
57. Theory Department Read File, c/o D. W. Ross, Institute for Fusion Studies, University of Texas at Austin, Austin, TX 78712
58. Theory Department Read File, c/o R. C. Davison, Director, Plasma Fusion Center, 167 Albany Street, Cambridge, MA 02139
59. Theory Department Read File, c/o F. W. Perkins, Princeton Plasma Physics Laboratory, P.O. Box 451, Princeton, NJ 08540
60. Theory Department Read File, c/o L. Kovrizhnykh, Lebedev Institute of Physics, Academy of Sciences, 53 Leninsky Prospect, Moscow, U.S.S.R. V312
61. Theory Department Read File, c/o B. B. Kadomtsev, I. V. Kurchatov Institute of Atomic Energy, P.O. Box 3402, Moscow, U.S.S.R. 123182
62. Theory Department Read File, c/o T. Kamimura, Institute of Plasma Physics, Nagoya University, Nagoya, Japan
63. Theory Department Read File, c/o C. Mercier, Euratom-CEA, Service de Recherches sur la Fusion Controlee, Fontenay-aux-Roses (Seine), France
64. Theory Department Read File, c/o T. E. Stringer, JET Joint Undertaking, Culham Laboratory, Abingdon, Oxon, OX14 3DB, England
65. Theory Department Read File, c/o K. Roberts, Culham Laboratory, Abingdon, Oxon, OX14 3DB, England
66. Theory Department Read File, c/o D. Biskamp, Max-Planck-Institut fur Plasmaphysik, D-8046 Garching bei Munchen, Federal Republic of Germany
67. Theory Department Read File, c/o T. Takeda, Japan Atomic Energy Research Institute, Tokai, Naka, Ibaraki, Japan
68. Theory Department Read File, c/o C. S. Liu, General Atomic Company, P.O. Box 81608, San Diego, CA 92138
69. Theory Department Read File, c/o L. D. Pearlstein, Lawrence Livermore National Laboratory, P.O. Box 808, Livermore, CA 94550
70. Theory Department Read File, c/o R. Gerwin, CTR Division, MS 640, Los Alamos National Laboratory, P.O. Box 1663, Los Alamos, NM 87545
71. J. D. Callen, Department of Nuclear Engineering, University of Wisconsin, Madison, WI 53706
72. R. W. Conn, Department of Chemical, Nuclear, and Thermal Engineering, University of California, Los Angeles, CA 90024
73. S. O. Dean, Director, Fusion Energy Development, Science Applications, Inc., 2 Professional Drive, Suite 249, Gaithersburg, MD 20760
74. H. K. Forsen, Bechtel Group, Inc., Research Engineering, P.O. Box 3965, San Francisco, CA 94105
75. R. W. Gould, Department of Applied Physics, California Institute of Technology, Pasadena, CA 94105

76. D. G. McAlees, Exxon Nuclear Company, Inc., 777 106th Avenue, NE, Bellevue, WA 98009
77. P. J. Reardon, Princeton Plasma Physics Laboratory, P.O. Box 451, Princeton, NJ 08540
78. W. M. Stacey, School of Nuclear Engineering, Georgia Institute of Technology, Atlanta, GA 30332
79. Bibliothek, Institut fur Plasmaphysik, D-8046 Garching bei Munchen, Federal Republic of Germany
80. Bibliothek, Institut fur Plasmaphysik, KFA, Postfach 1913, D-5170, Julich 1, Federal Republic of Germany
81. Bibliotheque, Service du Confinement des Plasmas, CEA, B.P. No. 6, 92 Fontenay-aux-Roses (Seine), France
82. Documentation S.I.G.N., Department de la Physique du Plasma et de la Fusion Controlee, Association EURATOM-CEA, Centre d'Etudes Nucleaires, B.P. 85, Centre du Tri, 38041 Grenoble, Cedex, France
83. Library, Centre de Recherches en Physique des Plasmas, 21 Avenue des Bains, 1007 Lausanne, Switzerland
84. Library, Culham Laboratory, UKAEA, Abingdon, Oxon, OX14 3DB, England
85. Library, FOM Institute voor Plasma-Fusica, Rijnhuizen, Jutphaas, Netherlands
86. Library, Institute for Plasma Physics, Nagoya University, Nagoya 464, Japan
87. Library, International Centre for Theoretical Physics, Trieste, Italy
88. Library, Laboratoria Gas Ionizzati, Frascati, Italy
89. Plasma Research Laboratory, Australian National University, P.O. Box 4, Canberra, ACT 2000, Australia
90. Thermonuclear Library, Japan Atomic Energy Research Institute, Tokai, Naka, Ibaraki, Japan
91. Library, Plasma Physics Laboratory, Kyoto University, Gokasho Uji, Kyoto, Japan
92. R. Varma, Physical Research Laboratory, Navangpura, Ahmedabad, India Institute of Physics, Academia Sinica, Peking, Peoples Republic of China
93. Office of the Assistant Manager for Energy Research and Development, Department of Energy, Oak Ridge Operations, Oak Ridge, TN 37830

94-265. Given distribution as shown in TID-4500, Magnetic Fusion Energy, (Distribution Category UC-20 g: Theoretical Plasma Physics)

ACKNOWLEDGMENTS

The authors would like to acknowledge useful discussions with Don Spong.

Research sponsored by the Office of Fusion Energy, U.S. Department of Energy, under contract W-7405-eng-26 with the Union Carbide Corporation.